TITLE: Transcriptome-wide association study of schizophrenia and chromatin activity yields mechanistic disease insights

AUTHORS: Alexander Gusev[1,2,*], Nick Mancuso[3], Hilary K Finucane[1,4], Yakir Reshef[5], Lingyun Song[6,7], Alexias Safi[6,7], Edwin Oh[8], Schizophrenia Working Group of the Psychiatric Genomics Consortium, Steven McCarroll[9,10], Benjamin Neale[2,10,11], Roel Ophoff[12,13], Michael C O'Donovan[14], Nicholas Katsanis[8], Gregory E Crawford[6,7], Patrick F Sullivan[15,16], Bogdan Pasaniuc[3,*,†] and Alkes L Price[1,2,*,†]

[1] *Department of Epidemiology, Harvard T.H. Chan School of Public Health, Boston, Massachusetts, USA.*
[2] *Program in Medical and Population Genetics, Broad Institute of MIT and Harvard, Cambridge, Massachusetts, USA.*
[3] *David Geffen School of Medicine, University of California, Los Angeles, Los Angeles, California, USA.*
[4] *Department of Mathematics, Massachusetts Institute of Technology, Cambridge, Massachusetts, USA.*
[5] *Department of Computer Science, Harvard University, Cambridge, Massachusetts, USA.*
[6] *Center for Genomic and Computational Biology, Duke University, Durham, North Carolina, USA.*
[7] *Department of Pediatrics, Division of Medical Genetics, Duke University Medical Center, Durham, North Carolina, USA.*
[8] *Center for Human Disease Modeling, Duke University Medical Center, Durham, North Carolina, United States.*
[9] *Department of Genetics, Harvard Medical School, Boston, Massachusetts, USA*
[10] *Stanley Center for Psychiatric Research, Broad Institute of MIT and Harvard, Cambridge, Massachusetts, USA*
[11] *Analytic and Translational Genetics Unit, Massachusetts General Hospital and Harvard Medical School, Boston, Massachusetts, USA.*
[12] *Center for Neurobehavioral Genetics, University of California, Los Angeles, Los Angeles, California, USA*
[13] *Department of Psychiatry, Brain Center Rudolf Magnus, University Medical Center Utrecht, Utrecht, The Netherlands*
[14] *MRC Centre for Psychiatric Genetics and Genomics, Cardiff University, Cardiff, UK*
[15] *Departments of Genetics and Psychiatry, University of North Carolina, Chapel Hill, North Carolina, USA*
[16] *Department of Medical Epidemiology and Biostatistics, Karolinska Institutet, Stockholm, Sweden*
∗*Corresponding authors*

†*Equal contribution*

ABSTRACT: Genome-wide association studies (GWAS) have identified over 100 risk loci for schizophrenia, but the causal mechanisms remain largely unknown. We performed a transcriptome-wide association study (TWAS) integrating expression data from brain, blood, and adipose tissues across 3,693 individuals with schizophrenia GWAS of 79,845 individuals from the Psychiatric Genomics Consortium. We identified 157 genes with a transcriptome-wide significant association, of which 35 did not overlap a known GWAS locus; the largest number involved alternative splicing in brain. 42/157 genes were also associated to specific chromatin phenotypes measured in 121 independent samples (a 4-fold enrichment over background genes). This high-throughput connection of GWAS findings to specific genes, tissues, and regulatory mechanisms is an essential step toward understanding the biology of schizophrenia and moving towards therapeutic interventions.

INTRODUCTION

1 Genome-wide association studies (GWAS) have yielded thousands of robustly associated variants for schizophre-
2 nia (SCZ) and many other complex traits, but relatively few of these associations have implicated specific
3 biological mechanisms [1,2], as GWAS association signals often span many putative target genes, may affect
4 gene expression through regulatory [3] or structural elements [4], and may affect genes at considerable genomic
5 distances via chromatin looping [5,6]. A growing body of research has demonstrated the enrichment of SCZ
6 GWAS risk variants and heritability within regulatory elements identified through maps of chromatin mod-
7 ifications and accessibility [1,7–13]. Since chromatin modifications are themselves under genetic control [6,14–19],
8 a causal mechanism for SCZ loci could lead from genetic variation to chromatin modifiers to gene expression
9 and finally to disease risk. Indeed, QTLs for chromatin (and other molecular phenotypes) are enriched within
10 GWAS associations, further supporting this hypothesis [6,18,20,21].

11 In this work, we leveraged large gene expression cohorts from multiple tissues, as well as splice variants in
12 brain, to perform a transcriptome-wide association study (TWAS) [22–24] in a large SCZ GWAS data set [1]
13 to identify genes whose expression is associated with SCZ and mediated by genetics. We subsequently
14 performed a TWAS for a diverse set of chromatin phenotypes to identify SCZ susceptibility genes that are
15 also associated with specific regulatory elements. To our knowledge, this is the first TWAS to integrate
16 analysis of gene expression, differential splicing, and chromatin variation, moving beyond top SNPs to
17 implicate SCZ-associated molecular features across the regulatory cascade (Figure 1A).

RESULTS

18 *TWAS for SCZ identifies new susceptibility genes*

19 We analyzed gene expression and genome-wide SNP array data in 3,693 individuals across four expression
20 reference panels spanning three tissues: RNA-seq from the dorsolateral prefrontal cortex (PFC) of 621
21 individuals - including SCZ and bipolar (BIP) cases and controls - collected by the CommonMind Consortium
22 (CMC) [25] (see Web Resources), expression array data measured in peripheral blood from 1,245 unrelated
23 individuals from the Netherlands Twin Registry (NTR) [26], expression array data measured in blood from
24 1,264 individuals from the Young Finns Study (YFS) [23], and RNA-seq measured in adipose tissue from
25 563 individuals from the Metabolic Syndrome in Men study (METSIM) [23]. The CMC/brain RNA-seq data
26 further allowed the characterization of differentially spliced introns [27] (see Methods). Average cis and trans
27 estimates of SNP-heritability of expression (h_g^2, see Methods) were highly significant in each panel, with
28 nominally significant cis-h_g^2 ($P < 0.01$) for a total of 18,084 genes summed across the four panels (10,819
29 unique genes; Table S1), as well as an additional 9,009 differentially spliced introns in brain (in 3,908 unique
30 genes; Table S1).

31 We performed a TWAS using each of the four gene expression reference panels and summary-level data from
32 the PGC SCZ GWAS of 79,845 individuals [1] in order to identify genes associated to SCZ (Figure S1). Briefly,
33 this approach integrates information from expression reference panels (SNP-expression correlation), GWAS
34 summary statistics (SNP-SCZ correlation), and LD reference panels (SNP-SNP correlation) to assess the
35 association between the cis-genetic component of expression and phenotype (expression-SCZ correlation) [23]
36 (Figure 1A). In practice, the expression reference panel was used as the LD reference panel, and cis SNP-
37 expression effect sizes were estimated using a sparse mixed linear model [28] (see Methods).

38 The TWAS identified 247 transcriptome-wide significant gene-SCZ and intron-SCZ associations (summed
39 across expression reference panels) for a total of 157 unique genes, including 49 genes that were significant
40 in more than one expression panel (Figure 2, Figure S1, Table 1, Table S2, S3). Of the 104 (non-HLA,
41 autosomal) known PGC GWAS loci [1], 47 loci overlapped with at least one TWAS gene locus (accounting
42 for 122/157 genes) with the remaining 35/157 genes implicating novel loci. We excluded the MHC region
43 (chr6:28-34MB) from our primary analyses due to its complex haplotype and LD structure. However, as
44 a positive control we specifically tested the *C4A* gene recently fine-mapped for SCZ [4], which lies inside the
45 MHC, and confirmed a highly significant TWAS association between *C4A* expression in brain tissue and
46 SCZ ($P = 1.8 \times 10^{-18}$). Across all TWAS associations, the implicated gene was the nearest gene to the top
47 SNP at the locus in only 56% of instances (using the 10,819 cis-heritable genes as background; decreasing

to 24% of instances when using all 26,469 known RefSeq genes), underscoring previous observations that the nearest gene to a GWAS hit is often not the most likely susceptibility gene when integrated with expression data[23,24,29,30]. Likewise, conditioning on the predicted expression of a TWAS-associated gene (using summary-level data[31], see Methods) reduced the χ^2 of the lead GWAS SNP at the locus (including genome-wide significant and non-significant loci) from 42 to 10 on average, and explained more of the association signal than conditioning on the corresponding top expression-QTL (eQTL) (Table S4). For the 43 lead GWAS SNPs at genome-wide significant loci that were in LD ($r^2 > 0.05$) with the predicted expression of at least one TWAS-significant gene (out of 47 overlapping index SNPs), joint conditioning on the predicted expression of all such genes reduced the median SNP P-value from $P = 1.2 \times 10^{-10}$ to $P = 0.028$ (Table S5). Given that the TWAS typically captures only 60-80%of the cis component of gene expression at these expression panel sample sizes[23], the complete elucidation of the cis component could potentially explain the entire GWAS signal at these loci.

For both total gene expression and differentially spliced introns, we frequently observed hotspots of multiple TWAS-associated genes in the same locus, a phenomenon previously observed for complex traits[30]. To quantify the total number of independently associated genes, we applied summary statistic-based approximate conditional and joint association methods[31] to identify genes/introns that had significant TWAS associations when analyzed jointly (see Methods). This yielded a set of 63 jointly significant associations, of which 17 were at novel loci (Table 1, Table S3). 8 loci contained multiple significant associations (spanning 16 genes) in the joint analysis, indicative of allelic heterogeneity. Differentially spliced introns in CMC/brain accounted for more jointly significant associations than any other reference panel (Table 1), followed by gene expression in brain, emphasizing the importance of having both expression and splicing measured in a relevant tissue.

The differentially spliced introns accounted for 46 transcriptome-wide significant gene associations (of which 10 were at novel loci), comparable to the 44 significant gene associations from brain (Table 1, Supplementary Materials), despite the fact that differentially spliced introns accounted for 30% fewer significantly cis-heritable genes than total expression (Table S1). Overall, 20/46 associations corresponded to genes that were not tested in the analysis of total gene expression due to non-significant expression heritability, and 19 of the remaining 26 did not have a transcriptome-wide significant association for total gene expression. We identified multiple TWAS loci driven by specific splice-QTL (sQTL) SNPs that significantly explained a SCZ GWAS association independent of the eQTL effects (Figure S2, S3, S4; Supplementary Materials). This is consistent with the recent observation that sQTLs are typically independent of eQTLs at the same gene[27]. We note that, in contrast to total gene expression, effect direction for these associations is difficult to interpret because multiple alternatively spliced exons within an isoform yielded excised introns that were highly negatively correlated.

This SCZ GWAS data[1] was recently evaluated in a TWAS with gene expression using Summary-based Mendelian Randomization (SMR)[24], identifying 16 transcriptome-wide significant associated genes (in contrast to 157 identified here). This gap could be explained by several differences in the methods: SMR relies on individual eQTL significance and a first stage association at the top eQTL, which has been previously shown to have less power than our TWAS approach using all SNPs in the locus[23]; the SMR test uses an intentionally conservative second stage test for heterogeneity; and the SMR analysis used a different expression panel from a meta-analysis of blood. Of the 16 gene associations identified by SMR, 12 were tested in our study in blood, all replicated at nominal $P < 0.05$ (with consistent sign), and 9 were transcriptome-wide significant - a striking concordance given the different methods and independent expression panels used.

TWAS associations replicate in internal and external SCZ cohorts

We first replicated the TWAS signal using internal cross-validation within the PGC SCZ GWAS cohorts[1] (we had permission to access individual genotypes for 58,246 of 79,845 samples). As a prerequisite step, we verified that TWAS using the raw GWAS data produced similar results as TWAS using summary statistics[23], observing a correlation of Z-scores ranging from 0.85-0.90 despite the somewhat different set of GWAS samples and independent measures of LD (Table S6). Next, we down-sampled the PGC data into GWAS discovery samples of various sizes (10,000-50,000) to quantify the power and out-of-sample replication of the SCZ TWAS associations (where the expression panel size was always held constant; Figure 3A). We estimated TWAS effect-size precision as the slope of a regression of replication vs. discovery TWAS effect sizes across

transcriptome-wide significant associations (see Methods), where a slope below 1 represents over-estimated effect sizes in the discovery data due to winner's curse. Across random down-samples, average effect-size precision was 0.93 at a discovery sample size of 50,000, indicating minimal winner's curse and projecting highly accurate effect-size estimates in the full TWAS. The number of transcriptome-wide significant associated genes increased linearly with GWAS sample size and was similar across all four expression reference panels (with more associations in brain expression at the largest discovery size), consistent with a polygenic architecture and many undiscovered associations.

We next replicated the TWAS associations externally using case-control phenotypes from the CMC cohort (which consisted of SCZ+BIP cases and controls; all cases were included due to the high genetic correlation between these two diseases[32]). We observed significant replication across all four expression panels, with effect-size precision not significantly different from 1 (Figure 3B; Figure S5). Surprisingly, the TWAS gene effect-sizes achieved a higher effect-size precision than GWAS SNP effect-sizes (Figure S6), possibly due to TWAS aggregating heterogeneous effects in a locus more effectively than a single top SNP. We note that even though the same CMC samples were used for the TWAS brain expression reference panel and replication using case-control status, this is an independent replication because CMC case-control status was never used in the discovery TWAS.

Gene-based risk scores are more predictive than top SNPs

Next, using all transcriptome-wide significant TWAS genes and differentially spliced introns identified in the PGC and their corresponding discovery effect sizes, we constructed gene-based risk scores (GeRS) from their predicted expression in the CMC (SCZ+BIP) case-control samples (see Methods). The GeRS from each expression panel were significantly associated to case-control status, with the strongest association coming from the CMC/brain expression GeRS, which explained $1.4\times$ more SCZ variance (and was more significant; $P = 2.0 \times 10^{-4}$ vs. 1.2×10^{-3}) than a genetic risk score computed using the 104 (non-HLA, autosomal) published genome-wide significant GWAS associations[1] (Figure 3C). The GeRS remained significant in a joint model with the published GWAS predictor ($P = 0.01$, Table S7) showing that the TWAS is prioritizing disease-relevant signal beyond the top SNPs.

We relaxed the significance threshold and found gene-based polygenic risk scores (GePRS) to be highly predictive across the full spectrum of TWAS association P-values (Figure 3D), as observed previously with SNP-based polygenic scores[1,33,34]. Although the prediction was significant in all tissues individually, there was evidence of increased effect in brain, with the prediction from brain (genes and introns) capturing 92% of the joint prediction from all tissues (Figure 3D; Figure S7). A GePRS from actual measured expression and differential splicing in brain was substantially less significant than the genetic GePRS (Figure S7), as expected if the non-genetic component of expression is independent of the TWAS signal. Based on polygenic theory[35,36], the best TWAS GePRS was estimated to account for 26% of the total SCZ SNP-heritability (see Supplementary Material), indicating a substantial contribution from cis effects in these four tissues.

We sought to investigate temporal differences within the CMC/brain TWAS signal using individual transcriptomes collected by the BRAINSPAN study (see Web Resources) across developmental periods in the same brain sub-region (PFC) ranging from fetal to adult. For each of 19 developmental periods, we estimated differential expression relative to the other periods as an indicator of temporal specificity. We observed TWAS χ^2 statistics to be significantly positively correlated with differential expression from the mid-fetal developmental period ($P < 0.05/19$), and corresponding significant negative correlation for differential expression from post-fetal periods (Figure S8, S9). The effect was most significant in the CMC/brain TWAS, less significant in the two blood TWAS, and non-significant in the adipose TWAS. This further underscores tissue-specific differences in the TWAS associations, and prioritizes genes expressed in early development for relevance to SCZ.

Chromatin TWAS identifies specific regulatory mechanisms for SCZ-associated genes

We next sought to identify relationships between the expression of associated genes from the SCZ TWAS and variation in cis-regulatory elements marked by chromatin (Figure 1A). We used population-level ChIP-Seq chromatin phenotypes measured in 76 HapMap YRI LCLs for H3k27ac (marking active enhancers),

H3k4me1 (enhancers), H3k4me3 (promoters), and DNAse (open chromatin)[6], and in 45 HapMap CEU LCLs for H3k27ac, H3k4me1, H3k4me3, PU1 (regulatory transcription factor) and RNA polymerase II (RPB2, associated with active transcription)[18]. For each of the nine chromatin phenotypes, sites with an excess of ChIP-Seq reads were categorized into local "peaks" corresponding to increased chromatin activity[6,18]. For each peak, the chromatin abundance across individuals was then treated as a single quantitative trait (with quality control mirroring the gene expression analyses; see Methods). Both cohorts additionally had gene expression measured by RNA-seq in the same samples, and we first used Haseman-Elston regression[37] to quantify the average genetic correlation between gene expression and all chromatin phenotype peaks in the cis locus, for all genes (see Methods). These cis genetic correlations were highly significant (and substantially higher than total correlation of measured phenotypes) across all chromatin phenotypes, persisting for peaks as far as 500kb from the TSS (Figure S10, S11, Table S8, see Methods). We also observed large and highly significant genetic correlations between peaks from different chromatin phenotypes (Figure S12), suggesting that such peaks may tag a single underlying biological feature.

Motivated by these findings, we applied individual-level TWAS methods[23] to predict expression from the much larger expression reference panels into samples with chromatin phenotypes and searched for expression-chromatin associations. Prediction was performed from expression to chromatin phenotype samples (instead of from chromatin phenotype to expression samples) due to improved numerical stability in the larger expression panels, but we note that this choice was agnostic to the direction of causality (See Supplementary Materials). We confirmed by simulation that this chromatin TWAS strategy is well-calibrated (Figure S13) and much better powered to identify SNP $\rightarrow$ chromatin $\rightarrow$ expression associations compared to the conventional approach of testing each SNP for a significant association to both expression (eQTL) and nearby chromatin peaks (cQTL)[6,18] (Figure 4A, Figure S14).

We performed the chromatin TWAS for the 10,819 significantly heritable genes and 9,009 differentially spliced introns analyzed in the SCZ TWAS, together with all chromatin peaks in the $\pm$500kb locus of each gene. Focusing on the 157 transcriptome-wide significant genes from the SCZ TWAS, we identified 42 genes (including 7 genes at novel loci) that also had Bonferroni significant chromatin TWAS associations (to a total of 78 individual chromatin peaks) in analyses using the same expression reference panel (Table 1, Table 2, Table S9, S10). Significant evidence of a chromatin-SCZ association was observed for the majority of genes using a separate TWAS-like test as well as the SMR[24] test using cQTLs, in spite of the low sample size (Supplementary Materials, Table S11). Individually, these 42 loci represent specific mechanistic hypotheses where the implicated chromatin phenotypes are disrupted and mediate the expression of susceptibility genes. Overall, there was a highly significant enrichment of gene-chromatin TWAS associations at SCZ TWAS genes relative to all heritable genes (OR=3.9; $P = 1.4 \times 10^{-11}$ by Fisher's exact test), suggesting that such mechanisms are particularly relevant for SCZ susceptibility genes. The enrichment was also individually significant ($P < 0.05/5$) for all tissues except adipose (Table 1). Surprisingly, the SCZ-associated differentially spliced introns were also enriched for chromatin associations (OR=5.0, $P = 8.1 \times 10^{-5}$), even though differentially spliced introns had many fewer chromatin associations overall (see below), suggesting that epigenetic regulation of splicing may be particularly relevant for SCZ susceptibility genes. Only 8 of the 78 chromatin peaks underlying joint SCZ TWAS and chromatin TWAS associations were within the promoter ($\pm$2kb of the TSS) of their associated gene. This suggests that most regulatory elements affecting SCZ are distally located, as previously observed in other traits[6,8,20] and underscores the importance of searching broadly around the TSS.

We describe three specific examples of TWAS associations to SCZ and chromatin phenotypes. First, the expression of $SLC45A1$ in CMC/brain was associated with SCZ ($P = 3.5 \times 10^{-8}$; overlapping a significant GWAS locus) as well as a distal RPB2 peak (106kb from TSS; $P = 1.5 \times 10^{-5}$), with significant marginal associations (QTLs) for both expression and chromatin (Figure 1B). TWAS prioritized this gene-peak combination from 15 genes and 60 peaks in the 1MB locus. Conditioning[31] on the predicted expression of $SLC45A1$ explained all significant eQTLs/cQTLs and GWAS SNPs in the locus. Notably, $SLC45A1$ was not the nearest gene to the top GWAS SNP nor to the associated chromatin peak, and the lead GWAS SNP was only nominally associated with the RPB2 peak. This highlights a chromatin association that could not have been identified using conventional approaches based on proximity or overlapping top hits. Second, the expression of $PPP2R3C$ in NTR/blood was associated with SCZ ($P = 3.4 \times 10^{-6}$) - despite no genome-wide significant SNPs at the locus - as well as two distal peaks for H3k4me1 (minimum $P = 1.0 \times 10^{-9}$) and

1 two distal peaks for H3k27ac (minimum $P = 4.1 \times 10^{-6}$) (Figure S15). The four chromatin peaks clustered
2 together physically and suggest a coordinated regulatory effect on expression. Conditioning on the predicted
3 expression of *PPP2R3C* again explained all significant marginal associations for the implicated phenotypes
4 (Figure S15). *PPP2R3C* was the nearest gene to the most significantly associated SNP at the locus and
5 to the implicated chromatin peaks. However, because the locus was not genome-wide significant, this as-
6 sociation would not have been identified in a conventional analysis of known GWAS loci. *PPP2R3C* was
7 also recently identified by SMR analysis of SCZ in an independent expression panel[24]; our findings identify
8 specific chromatin features for experimental follow-up. Third, we describe the *MAPK3* locus in detail below.

9 *Allelic imbalance analyses localize TWAS association for MAPK3*

10 We highlight the SCZ TWAS association of *MAPK3* expression in CMC/brain ($P = 1.3 \times 10^{-06}$), over-
11 lapping a significant SCZ GWAS locus. Notably, *MAPK3* is located inside the 16p11 copy number variant
12 that has been associated with SCZ and autism[38–41], and has recently been linked with differential protein
13 abundance in SCZ[42] and shown to respond to pharmacological targeting in cultured neurons[43]. In our anal-
14 ysis, *MAPK3* was also nominally differentially expressed in the independent CMC (SCZ+BIP) case-control
15 samples (Wilcoxon $P = 0.03$, over-expressed in controls) despite the small sample size. The chromatin
16 TWAS identified associations between *MAPK3* and two peaks near the TSS (H3k27ac, $P = 7 \times 10^{-6}$;
17 RPB2, $P = 1 \times 10^{-11}$). In the CEU chromatin phenotype samples, where *MAPK3* expression was also
18 measured in LCLs, the H3k27ac and RPB2 peaks explained 36% ($P = 7 \times 10^{-6}$) and 23% ($P = 5 \times 10^{-4}$) of
19 the variance in measured expression, respectively, with only the H3k27ac peak significant in a joint model.
20 Because the chromatin TWAS associations were identified in LCLs, we examined additional epigenetic data
21 from H3k27ac, H3k4me3 and ATAC-seq measured in brain tissues (including pre-frontal cortex) as part
22 of the PsychENCODE project[44] and showed the presence of peaks across all three chromatin phenotypes
23 (Figure S16, Supplementary Materials). Strikingly, both peaks were also nearly identical to two recently
24 identified human-gained neuro-developmental enhancers in independent fetal cortex tissues[45] (Figure S16),
25 providing compelling evidence of evolutionary importance. We then focused on two putatively functional
26 SNPs within the ATAC-seq peak (rs28529403 and rs61764202, in tight LD with $\rho = 0.7$) that were both
27 recently classified as disrupting multiple transcription factor binding sites[21] and therefore plausible causal
28 variants. Conditioning on either SNP accounted for all significant marginal associations across the corre-
29 sponding expression and chromatin phenotypes (Figure S17, S18), consistent with these SNPs driving the
30 local signal.

31 We sought to confirm the effect at these SNPs by looking at allelic imbalance, which naturally accounts for
32 environmental differences across individuals[46,47]. First, we focused on allele-specific expression in the CMC
33 RNA-seq data (which is statistically independent of the QTL-based signal used for TWAS). We phased
34 the locus and, for each SNP, tested all heterozygous carriers for an imbalance in RNA-seq reads at the
35 transcript SNP (see Methods). Both putative SNPs showed significant evidence of allele-specific expression
36 (rs28529403, $P = 2.5 \times 10^{-21}$; rs61764202, $P = 2.0 \times 10^{-21}$), and were the most significantly imbalanced in
37 the locus (Table S12, Figure S19).

38 Next, we collected additional ATAC-seq data at this locus, for a total of 314 CMC individuals[44], and looked
39 for allele-specific chromatin activity in the same manner. We restricted to 267 SNPs that were Bonferroni
40 significant for allele-specific expression (above), and tested all heterozygous carriers for an imbalance in
41 ATAC-seq reads using either of the two peak SNPs as anchors (see Methods). We observed a Bonferroni
42 significant allelic imbalance at rs61764202 (94 heterozygous samples, $P = 8.6 \times 10^{-5}$), which was more signif-
43 icant than any other SNP in phase with rs61764202; we did not observe significant imbalance at rs28529403
44 (100 samples, $P = 0.15$) or any other SNP in phase with rs28529403 (Table S12). The imbalance was also
45 individually significant in four samples but with opposite direction in one of the four (Figure S20, Table S13).
46 For this sample, we cannot decisively rule out the possibility of artifact, a mis-imputed heterozygous call,
47 confounding from an interaction involving nearby features, or tissue sub-type heterogeneity. However, such
48 biases would not be expected to inflate the combined test across all individuals. Taken together, the allele-
49 specific signal from both molecular phenotypes nominates the alternative allele at rs61764202 as disrupting
50 chromatin activity, increasing *MAPK3* expression, which in turn decreases SCZ risk.

Chromatin TWAS associations explain the bulk of cis expression regulation

We expanded the chromatin TWAS to all 10,819 heritable genes (not just SCZ-associated genes) in order to evaluate the properties of all chromatin TWAS associations. This yielded roughly $7\times$ more Bonferroni significant expression-chromatin associations than using the conventional in-sample eQTL/cQTL overlap approach[6,18] (Figure 4B, Table S14), consistent with our previous simulations. Across all tissues, 806 unique genes had a transcriptome-wide significant association (see Methods) with at least one chromatin phenotype (Figure 4B, Table S15), and 4,294 genes were significant at the 10% (per-phenotype) FDR used in previous studies[6,18] (Table S16). In contrast, only 224 of 9,009 differentially spliced introns in the CMC has a transcriptome-wide significant association with a nearby chromatin mark, corresponding to 2-3$\times$ fewer associations than identified using total CMC gene expression (depending on the chromatin phenotype, Table S17). As expected, the distribution of associated chromatin peaks was centered at the TSS of the corresponding gene (Figure S21). However, additional associations were consistently observed when testing distal peaks (> 10kb) after correcting for the additional tests performed, in contrast to the results from eQTL/cQTL overlap (Figure 4B, S22, S23). We evaluated these distal chromatin TWAS associations against genome-wide Hi-C measured in a reference LCL[6], reasoning that truly interacting gene-peak pairs are likely to be in 3-dimensional chromatin contact. Across all chromatin phenotypes, we found distal (≥ 10kb) gene-peak associations to be significantly enriched for Hi-C inferred loops relative to random (distance-matched) gene-peak pairs, with an odds ratio of 2.4 (95% CI 2.2-2.5; $P < 1 \times 10^{-16}$) for pairs up to 500kb apart (Figure S24).

Our primary analyses leveraged external expression data in larger sample sizes, but we also analyzed directly measured expression in chromatin samples for validation. First, we confirmed that the predicted expression was significantly correlated with measured expression in the chromatin samples (Table S18). Even though the four expression reference panels all contained samples of European ancestry, this correlation was significant for both CEU and YRI target samples; with average R^2 for YRI half as large as for CEU, providing an estimate of the power loss due to differences in linkage disequilibrium (LD) patterns across populations[48]. Next, for every TWAS-associated gene-chromatin peak pair, we measured the association between actual measured expression and the corresponding chromatin phenotype. If the chromatin TWAS association reflects true genetic correlation, we would expect the measured expression to also be highly correlated (barring tissue-specific differences between the expression panels). Indeed, across the 806 chromatin TWAS-associated genes, the correlation between measured expression and an associated chromatin phenotype was highly significant when compared against a distance-matched background null (Figure S10B). In CEU, where cross-population LD differences are minimized, the average individual TWAS-associated chromatin peak explained 21% of the variance in measured expression of its target gene for peaks within 2kb of the TSS, with the subset of distal peaks (2kb-500kb to the gene boundary, 32% of the peaks) explaining 18% (Figure S25, S26, S27, S28). This strikingly high variance explained is comparable to the total cis-h_g^2 of these genes (in blood, the tissue type most relevant to LCL; Table S19), implying that the cis-genetic effect on expression may be fully explained by individual chromatin TWAS peaks. We stress that the measured expression in chromatin samples was completely independent of the external expression data used in the chromatin TWAS, ensuring that these estimates were not biased by over-fitting or winner's curse. For the three chromatin phenotypes that were measured in both CEU and YRI, associated peaks identified in one population were still predictive of association with measured expression in the other (Figure S29, S30, Table S20), lending further support to previous observations that regulatory activity and the resulting impact on disease is stable across ethnicities[16,49] and supporting our use of measurements from multiple populations.

Chromatin modifications mediate SNP-expression associations that impact SCZ

We next evaluated whether the SCZ and chromatin TWAS associated loci were more consistent with a chromatin mediating (SNP $\rightarrow$ chromatin $\rightarrow$ expression) or expression mediating (SNP $\rightarrow$ expression $\rightarrow$ chromatin) causal model leading to SCZ susceptibility. We derived a statistic based on the ratio of cis-genetic covariance (cov_g) between SCZ and the two molecular phenotypes (see Methods). Conceptually, the genetic effect of a given molecular phenotype on SCZ will be attenuated by environmental noise, which will manifest itself as lower cov_g to SCZ for phenotypes further along the molecular cascade. We estimated expression-SCZ and chromatin-SCZ cov_g in the CEU and YRI samples with both chromatin and expression

1   data, using cross-trait LD score regression[50]. Averaging across the 42 chromatin TWAS associations at
2   genes identified in the SCZ TWAS, both the expression-SCZ and chromatin-SCZ cov_g were significantly
3   higher than that of a random background of gene-peak pairs less than 500kb apart, with chromatin-SCZ
4   cov_g $2.5\times$ greater on average than expression-SCZ cov_g and more significantly different from the background
5   (Figure S31, see Methods). This corresponds to the chromatin phenotype explaining 35% of the variance in
6   expression under the model where it is the mediator, with the rest due to environmental or trans variance
7   independent of disease (see Methods). Furthermore, regressing the chromatin phenotype out of expression
8   led to non-significant estimates of expression-SCZ cov_g, but regressing the measured expression out of the
9   chromatin phenotype did not significantly affect the chromatin-SCZ cov_g estimates (Figure S31B). Both
10   observations strongly support a chromatin mediating model (SNP $\rightarrow$ chromatin $\rightarrow$ expression) previously
11   hypothesized[15–17], and extend it to SCZ etiology.

DISCUSSION

12   The landmark PGC SCZ GWAS paper stated that "if most risk variants are regulatory, available eQTL
13   catalogues do not yet provide power, cellular specificity, or developmental diversity to provide clear mech-
14   anistic hypotheses for follow-up experiments"[1]. In this work, we apply cutting-edge methodology to data
15   from expression and chromatin activity to provide mechanistic hypotheses. Applying the TWAS approach
16   to SCZ, we identified 157 unique genes with transcriptome-wide significant associations, whose predicted
17   expression explained the bulk of the corresponding GWAS SNP association. Genes below the transcriptome-
18   wide significance threshold continued to be strongly associated with SCZ and exhibited clear preference for
19   expression and splicing in the brain (though this can also reflect expression data quality). Indeed, alterna-
20   tive splicing in the brain yielded the greatest number of independent TWAS associations, highlighting an
21   important source of disease-relevant variation[27] with potential therapeutic implications[51,52]. 42 of the SCZ-
22   associated genes were significantly associated with nearby chromatin variation (a 4-fold enrichment relative
23   to non-SCZ genes), implicating specific regulatory features for functional follow-up. Our analyses strongly
24   supported a model where chromatin variation (likely marking differences in transcription-factor binding)
25   mediates the relationship between genetics and expression[15–17], and connect this model with SCZ etiology.
26   This may explain the modest overlap between eQTLs and GWAS hits previously reported[29,30,46], where
27   the downstream nature of the expression phenotype (relative to chromatin) would decrease power for such
28   overlap analyses.

29   We note several limitations and future directions of this study. First, the discovery chromatin phenotypes
30   analyzed here were measured in LCLs, preventing us from identifying regulatory elements that were brain-
31   specific and of potentially greater relevance to SCZ. Second, although TWAS is not confounded by reverse-
32   causality (disease $\rightarrow$ expression), instances where a SNP influences SCZ which in turn influences gene
33   expression (or the same SNP influences SCZ and expression independently) are statistically indistinguishable
34   from causal susceptibility genes. Therefore, although we can conclude that 26% of the SCZ h_g^2 is explained by
35   predicted expression of all genes analyzed here we cannot estimate the fraction that is truly causal without
36   further mediation experiments. Finally, our simulations indicate that the chromatin TWAS approach will
37   have substantially greater power as chromatin sample sizes increase into the hundreds[44]. As tissue acquisition
38   may be the biggest hurdle for producing larger data sets, methods that do not depend on measurements
39   from the same samples will remain critical. Above and beyond specific mechanistic findings for SCZ, our
40   findings outline a systematic approach to identify biological mediators of complex disease.

WEB RESOURCES

1 TWAS results:
2 `http://sashagusev.github.io/chromatinTWAS/`

3 TWAS methods:
4 `http://bogdan.bioinformatics.ucla.edu/software/twas/`

5 BRAINSPAN transcriptomes:
6 `http://www.brainspan.org/static/download.html`

7 CommonMind consortium:
8 `https://www.synapse.org/cmc`

9 Grubert et al data:
10 `http://chromovar3d.stanford.edu`

11 PGC summary data:
12 `https://www.med.unc.edu/pgc/downloads`

13 PLINK:
14 `https://www.cog-genomics.org/plink2`

15 PsychENCODE knowledge portal:
16 `https://www.synapse.org/#!Synapse:syn4921369/wiki/235539`

17 SNPWeights for principal component analysis:
18 `http://www.hsph.harvard.edu/alkes-price/software/`

19 Waszak et al data (provided by the authors):
20 `http://gardeux-vincent.eu/Cell2015/description.peaks.zip`,
21 `http://gardeux-vincent.eu/Cell2015/quantified.peaks.zip`,
22 `http://gardeux-vincent.eu/Cell2015/quantified.peaks.PEER.centered.zip`

39 The data reported in this paper are tabulated in the Supplementary Materials and archived at:
40 `http://sashagusev.github.io/chromatinTWAS/`

METHODS

1   *Data and quality control*

2   Genotypes and expression from the NTR[26], YFS[23], and METSIM[23] were processed as described in ref[23]
3   and the corresponding expression weights were downloaded directly from the TWAS web-site (see Web
4   Resources). Genotypes and expression data from the CMC[25] were processed using the GTEx Consortium
5   guidelines for eQTL analysis of RNA-seq data. Specifically, RNA-seq RPKM was quantile normalized across
6   samples; genes having > 10 individuals with zero reads were removed; each gene was rank-normalized; 15
7   PEER factors were computed; and the residual expression used.

8   We used the LeafCutter algorithm[27,53] to quantify de novo intron excision in the CMC RNA-seq data by
9   clustering reads that spanned intron junctions. These clusters correspond to individual isoforms and enable
10 an estimate of differential intron splicing computed from the ratio of reads spanning an intron relative to the
11 total isoform read count. Splice variants were quantified using LeafCutter default parameters: a minimum
12 of 50 reads per cluster, and a maximum intron length of 500kb. Based on the guidelines in ref.[53], the
13 following quality controls were applied to the inferred isoform clusters: clusters having > 10 individuals
14 with zero reads were removed; clusters with < 100 individuals having > 20 reads were removed; and introns
15 with < 5 individuals having non-zero counts were removed. The inferred per-sample abundance for each
16 intron was then treated as a molecular phenotype, normalized, and PEER-corrected as with total expression
17 above. This process identified 123,480 differentially spliced introns, of which 99,562 mapped to canonical
18 gene introns. We treated the differential splicing of these 99,562 introns as quantitative traits in the same
19 manner as total expression.

20 For genotype data, individuals failing a sex check or having 5% missing SNPs were removed. Additionally,
21 SNPs were removed if they had $> 5\%$ missing calls; $P < 0.05$ case-control missing association; $P < 5 \times 10^{-6}$
22 Hardy-Weinberg disequilibrium; $P < 5 \times 10^{-3}$ association to batch; $P < 5 \times 10^{-8}$ missing haplotype
23 association; or frequency $< 1\%$. Principal components (PCs) were computed using all samples for the NTR,
24 YFS, and METSIM data directly and using SNPweights (v2.1)[54] for the CMC data, outliers were removed
25 (samples > 6 standard deviations away the mean along any top component), and PCs included as fixed-
26 effects in estimating h_g^2. For all datasets, related individuals with GRM values > 0.05 were also removed
27 prior to estimating h_g^2.

28 h_g^2 *estimation*

29 Cis and trans h_g^2 were estimated using variance-components, modeling the phenotype as a multi-variante
30 Normal $y \sim \sigma^2_{g,cis} K_{cis} + \sigma^2_{g,trans} K_{trans} + \sigma^2_e I$ where K are the standard genetic relatedness matrices from
31 SNPs in the cis locus (K_{cis}) and in the rest of the genome (K_{trans}). The σ^2 parameters were fit for each
32 gene using AI-REML as implemented in the GCTA software[55], with principal components and sex included
33 as fixed effects. For h_g^2 of differentially spliced introns, the intron ratios condition out isoform abundance
34 but total gene expression was also included as a covariate to account for any residual correlation. As in
35 previous studies[26], individual estimates outside the plausible 0-1 range were allowed in order to achieve
36 unbiased mean estimates. The standard error of each estimate was approximated as the standard deviation
37 divided by the square root of the number of genes tested; however, significant differences were confirmed by
38 permutation tests (see below).

39 To evaluate the contribution of low-frequency variants, we imputed the NTR data to the Haplotype Reference
40 Consortium reference, yielding high-quality imputed SNPs down to MAF of 0.001. On average, we did not
41 observe a significantly non-zero contribution of imputed rare variants to cis-h_g^2, nor did we see a significant
42 change in common cis-h_g^2 due to denser imputation relative to array SNPs (Table S1). Though recent work
43 has identified biases in estimates of h_g^2 from rare variants[56], we expect these biases to be small in the cis
44 region and largely mitigated by the two-component model. We did not further evaluate the contribution of
45 rare variants to trans-h_g^2. No difference was observed when using dosages to construct the cis GRM.

46 In the CMC data, where SCZ/BIP and control status was also available, the average cis-genetic correlation
47 of expression between (SCZ/BIP) cases and controls was 1.00 (s.e. 0.02), indicating consistent direction of
48 eQTL effect sizes between cases and controls and motivating us to use the full cohort as a TWAS reference

1   panel (Table S21). We additionally performed multiple analyses of expression heritability associated with
2   functional category (Supplementary Materials) demonstrating pervasive enrichment of chromatin marks
3   near significantly heritable genes and underscoring the importance of chromatin variation to expression
4   heritability[57].

5   *Schizophrenia TWAS*

6   We analyzed publicly available schizophrenia summary statistics from the PGC GWAS of 79,845 individuals[1]
7   (see Web Resources). Summary statistic-based TWAS was performed as described previously[23] using cis
8   SNP-expression effect sizes computed by the BSLMM software[28] for each of the four expression reference
9   panels. Strand-ambiguous alleles (A/T, G/C) were removed from the summary data and all SNPs were set
10   to the same strand. We evaluated TWAS predictions using either the SNPs genotyped in each expression
11   reference panel, or imputed HapMap3 SNPs (which typically represent well-imputed SNPs). To account
12   for multiple hypotheses, we applied Bonferroni correction within each expression panel that was used. This
13   threshold was chosen so as to maximize consistency with previous published results and not penalize for
14   additional (and often highly correlated) expression panels tested. Specifically, we report "transcriptome-
15   wide" significance after correcting for the number of genes tested within each of the five reference panels
16   (CMC, CMC-splicing, NTR, YFS, METSIM; 5,419 tests on average). This is consistent with the correction
17   applied in previous TWAS results of multiple expression references[23].

18   To ensure that results from the CMC data were not biased by ascertainment for SCZ/BIP cases, we performed
19   a separate TWAS in which cis SNP-expression effect sizes were stratified on CMC case-control status and
20   meta-analyzed; we observed no significant differences compared to using the full sample (Table S22).

21   Conditional and joint analysis was performed using the summary statistic-based method described in ref.[31],
22   which we applied to genes instead of SNPs. This approach requires marginal association statistics (i.e. the
23   main TWAS results) and a correlation/LD matrix to evaluate the joint/conditional model. The correlation
24   matrix was estimated by predicting the cis-genetic component of expression for each TWAS gene using the
25   CMC genotypes and computing Pearson correlations across all pairs of genes. The 247 transcriptome-wide
26   significant TWAS associations across four reference panels (spanning 157 unique genes) were then added
27   to the model one at a time and retained if their conditional TWAS association remained significant after
28   Bonferroni correction for 247 tests. The same procedure was used to perform TWAS joint/conditional
29   analysis of marginal SNP/QTL associations.

30   *Schizophrenia TWAS replication within PGC2*

31   We used the individual-level PGC data[1] to perform replication analyses and compare to summary-based
32   results. Cis SNP-expression effect sizes were computed using the BSLMM software (as above) and pre-
33   dicted into each PGC sub-cohort to produce individual-level gene expression predictions. To evaluate the
34   importance of SNP platform, two separate analyses were performed for the CMC, using all genotyped SNPs
35   in the expression reference and all imputed HapMap3 SNPs, respectively. Association between predicted
36   expression and SCZ was assessed using logistic regression with sub-cohort label and 10 principal components
37   included as covariates. For the sub-sampling analysis, the full study was randomly split into discovery and
38   replication. The association was then measured in discovery samples only, and any significant genes again
39   tested for association in the replication samples. For sub-cohort analysis, one cohort was removed at a time
40   (marked as replication) and the same process repeated.

41   *Gene-based risk scores*

42   We adopted SNP-based polygenic risk score analysis[33] to evaluate TWAS predictive accuracy and validation.
43   Given a 1-by-M vector z of signed association statistics in the discovery study and an N-by-M matrix X
44   of genetic values for the corresponding M genes in the replication study, we constructed a gene-based risk
45   score $S = Xz$. The M genes were either all transcriptome-wide significant genes (gene risk score - GeRS) or
46   all genes passing relaxed p-value thresholds (gene polygenic risk score - GePRS). This risk score was then
47   tested against case/control status by a standard linear model $y \sim S + P + e$ where S is the risk score and P
48   is a matrix of principal components accounting for ancestry. The risk-score accuracy was then measured as

1   the R^2 from the above model less the R^2 from the model $y \sim P + e$ to account for ancestry, and converted
2   to the liability scale assuming a prevalence of 1%.

3   For the TWAS using METSIM, YFS, and NTR expression reference panels, the cis-genetic component of
4   expression was predicted in CMC samples. For the TWAS using the CMC expression panel, either the total
5   expression was used (Figure S7) or the cis-genetic component of expression was estimated directly using
6   BSLMM (equivalent up to a scaling factor to estimating genetic values by dropping each individual in turn).
7   We stress that the case/control label from the CMC data was never used to identify the TWAS associations,
8   and that the GeRS or GePRS from the CMC expression panel were thus evaluated against an independent
9   CMC case/control phenotype. Ascertaining cases in the CMC expression panel may increase the frequency of
10   causal variants and make the prediction more accurate than using a randomly ascertained expression panel,
11   however, we observed little difference when performing the TWAS using an expression panel consisting of
12   CMC controls only (Table S22).

13   *Power simulations for chromatin TWAS*

14   Using real genotypes from the UK10K[58] study, we simulated a model where SNPs X are causal for a
15   chromatin peak ($C = X\beta_X + e_C$) and chromatin is causal for expression ($E = C\beta_C + e_E$). 100 1MB loci
16   were randomly selected across the genome, and causal SNPs in each locus were then randomly selected from
17   common variants (MAF > 1%). Environmental noise was set such that SNPs explain 30% of the variance in a
18   chromatin peak, and chromatin explains 30% of the variance in expression (consistent with our observations
19   that expression h_g^2 is ∼ 10%). The TWAS was then performed using cis SNP-expression effect sizes computed
20   by BSLMM either predicting the chromatin phenotype (with increasing sample size) into 1,000 independent
21   individuals with expression or vice versa, and then performing an association between the predicted and
22   measured phenotype. Separately, eQTL and cQTL association was computed for every common SNP in the
23   locus using individuals with both expression and chromatin measured. To evaluate power at genome-wide
24   significance, a TWAS association was reported as significant if it had $P < 0.05$ after correcting for (average
25   30 peaks per locus) × (20,000 genes) = 600,000 tests. For the QTL-based approach, given M SNPs in
26   the locus, a SNP was reported as significant if it had an eQTL $P < 0.05$ after correcting for $M \times 20,000$
27   tests and a cQTL $P < 0.05$ after correcting for $M \times 30 \times 20,000$ tests. For a given chromatin sample
28   size, the simulation was then performed at 100 random loci and 5 random seeds each, with the fraction
29   of loci reported as significant by each method taken as the power (Figure S14). The TWAS simulation
30   was separately performed under the null, using non-heritable chromatin and expression, and shown to be
31   well-calibrated under the null (Figure s13).

32   *Individual-level chromatin TWAS*

33   We used cis SNP-expression effect sizes computed by BSLMM scores in the four expression reference panels
34   (including differentially spliced introns) to predict individual-level expression in the 45 CEU[18] and 76[6] YRI
35   individuals with measured chromatin phenotypes. We retained only SNPs that were typed in both studies
36   and removed strand-ambiguous SNPs. We did not perform any additional QC of the functional features,
37   which were all previously PEER-adjusted and normalized[6,18]. We note that even though the YRI target
38   samples are of different ethnicity, this prediction does not require an LD-reference panel and is therefore
39   only expected to suffer loss in power (but not increased type I error) due to the differences in LD. For each
40   predicted gene, we identified all chromatin peaks within a given window of the TSS (primary results used
41    $\pm 500 kb$) and tested each mark for association to predicted expression by linear regression.

42   *Multiple hypothesis correction for chromatin TWAS*

43   The large number of correlated phenotypes analyzed - expression from five experiments and chromatin from
44   nine experiments in two populations - allows for several approaches to multiple testing correction. For
45   the chromatin TWAS, we corrected for the number of gene-peak pairs tested within a single expression
46   reference and chromatin phenotype experiment (for example, number of gene-peak pairs when evaluating
47   predicted CMC expression with the CEU:H3k27ac chromatin phenotype). This is directly comparable to
48   the experiment-wide corrections applied in previous eQTL/cQTL analyses[6,18]. The same correction was

applied for the SCZ/chromatin TWAS overlap: for example, the 44 SCZ TWAS genes identified using CMC expression were within 500kb of 1,528 total peaks in the CEU:H3k27ac experiment and "overlap" was reported for any peak that had a chromatin TWAS association $P < 0.05/1,528$.

For comparison, we separately calculated the number of associations that were significant at 5% FDR across all molecular experiments. This yielded approximately $3.5\times$ more chromatin TWAS associations and $1.2\times$ more SCZ and chromatin TWAS associations (Table S2), demonstrating that the above experiment-wide Bonferroni correction strategy corresponds to a conservative study-wide FDR.

eQTL/cQTL overlap analysis

We compared the chromatin TWAS to the traditional approach of identifying SNPs that are significant both as cQTLs and eQTLs in real data (Figure 4B). For each population and given distance to TSS, we performed this analysis in two stages. Stage 1: We identified all eQTLs that were significant after Bonferroni correction for the total number of SNP-gene pairs tested. When distance to TSS was the maximal allowed (500kb), this resulted in 355 eQTLs in the YRI and 579 eQTLs in the CEU data. Stage 2: From the set of significant eQTLs, we then looked for those that were also significantly associated with peaks from a given chromatin phenotype (for peaks within the given distance to TSS), after Bonferroni correction for the number of eQTL-peak pairs tested. In both stages the tests were only counted for the given chromatin phenotype (e.g. H3K27ac in CEU). This was compared to the chromatin TWAS analysis where each gene was tested against any peak within the given distance, and number of significant results reported after Bonferroni correction for total number of gene-peak pairs tested.

Analysis of allele-specific expression

For each molecular phenotype (RNA-seq/ATAC-seq), we phased the locus using EAGLE2[59] and evaluated haplotype allelic imbalance as follows. Given a "peak" SNP (for which there are RNA/ATAC-seq reads) and a "target" SNP (for which we want to evaluate allelic imbalance) we restricted to individuals that were heterozygous for both SNPs and counted the number of peak reads mapping to the REF/ALT haplotypes of the target SNP. We then assessed statistical significance for deviation from 50% balance using a binomial test. When the peak SNP and target SNP are identical, this is equivalent to a standard allelic-imbalance test across all heterozygous carriers in the peak. Duplicate reads were removed using samtools prior to all analyses and only variants with ≥ 10 reads at the peak SNP were tested. See Supplementary Materials for details on individual phenotypes analyzed.

Ratio of cis-genetic covariance between chromatin-SCZ and expression-SCZ

To shed more light on the potential causal model, we sought to evaluate the evidence in support of two models of mediation: M_{CH}, where SNP $\rightarrow$ chromatin $\rightarrow$ expression $\rightarrow$ disease; and M_{EX}, where SNP $\rightarrow$ expression $\rightarrow$ chromatin $\rightarrow$ disease. Under the assumption of linear, additive variance across molecular phenotypes, this can be estimated via the ratio of genetic covariance (cov_g) between chromatin-SCZ and expression-SCZ. The fraction of environmental variance on expression (env_{EX}) under each model of mediation can then computed from the following equation (see Supp. Note for derivation):

$$cov_{g,\mathrm{CH}}/cov_{g,\mathrm{EX}} = 1/\sqrt{1 - env_{EX}^2}$$

To compare these two models without bias from sample size or assay, we estimated the genetic covariance (cov_g) using the PGC SCZ summary statistics and molecular data from the CEU/YRI individuals which had both chromatin and gene expression measured. For each SCZ/chromatin TWAS gene, we defined the target locus as ± 50kb of the union of gene and peak boundary and estimated SCZ-chromatin and SCZ-expression cov_g using cross-trait LD score regression[50], restricting to the well-imputed HapMap3 SNPs and using in-sample LD. To estimate significance, background cov_g was computed using the same procedure over 200 randomly gene-peak pairs within 500kb of the TSS. The observed and background estimates were then compared using the non-parametric Kolmogorov-Smirnov test. We note that for the YRI samples LD in the GWAS summary statistics is expected to differ from LD in the eQTL/cQTL data, and confound the raw

1   estimate of cov_g; however, because the random gene-peak pairs are also computed from the same population,

2   we do not expect significance measured against this null to be inflated. We separately considered a partial

3   correlation analysis, where each expression measurement was transformed to the residual of the associated

4   chromatin peak in a standard linear regression (and likewise for each chromatin measurement). The two

5   estimates of cov_g were again computed from these partial phenotypes as described above. We caution that

6   the estimate of e in the above equation was computed from an average across all loci, and could also be

7   consistent with confounding from different levels of measurement error for ChIP-seq and RNA-seq, a mixture

8   of models M_{CH} and M_{EX} that favors model M_{CH}, or mediation by other unobserved molecular phenotypes.

Bibliography

[1] Schizophrenia Working Group of the Psychiatric Genomics Consortium. (2014). Biological insights from 108 schizophrenia-associated genetic loci. Nature *511*, 421–427.

[2] Price, A. L., Spencer, C. C., and Donnelly, P. (2015). Progress and promise in understanding the genetic basis of common diseases. In Proc. R. Soc. B volume 282 The Royal Society pp. 20151684.

[3] Soldner, F., Stelzer, Y., Shivalila, C. S., Abraham, B. J., Latourelle, J. C., Barrasa, M. I., Goldmann, J., Myers, R. H., Young, R. A., and Jaenisch, R. (2016). Parkinson-associated risk variant in distal enhancer of α-synuclein modulates target gene expression. Nature *533*, 95–99.

[4] Sekar, A., Bialas, A. R., de Rivera, H., Davis, A., Hammond, T. R., Kamitaki, N., Tooley, K., Presumey, J., Baum, M., Van Doren, V., et al. (2016). Schizophrenia risk from complex variation of complement component 4. Nature *530*, 177–183.

[5] Claussnitzer, M., Dankel, S. N., Kim, K.-H., Quon, G., Meuleman, W., Haugen, C., Glunk, V., Sousa, I. S., Beaudry, J. L., Puviindran, V., et al. (2015). Fto obesity variant circuitry and adipocyte browning in humans. New England Journal of Medicine *373*, 895–907.

[6] Grubert, F., Zaugg, J., Kasowski, M., Ursu, O., Spacek, D., Martin, A., Greenside, P., Srivas, R., Phanstiel, D., Pekowska, A., et al. (2015). Genetic control of chromatin states in humans involves local and distal chromosomal interactions. Cell *162*, 1051–1065.

[7] Maurano, M. T., Humbert, R., Rynes, E., Thurman, R. E., Haugen, E., Wang, H., Reynolds, A. P., Sandstrom, R., Qu, H., and Brody, J. (2012). Systematic localization of common disease-associated variation in regulatory dna. Science *337*, 1190–1195

[8] Trynka, G., Sandor, C., Han, B., Xu, H., Stranger, B. E., Liu, X. S., and Raychaudhuri, S. (2013). Chromatin marks identify critical cell types for fine mapping complex trait variants. Nature Genetics *45*, 124–130.

[9] Pickrell, J. K. (2014). Joint analysis of functional genomic data and genome-wide association studies of 18 human traits. The American Journal of Human Genetics *94*, 559–573.

[10] Gusev, A., Lee, S. H., Trynka, G., Finucane, H., Vilhjálmsson, B. J., Xu, H., Zang, C., Ripke, S., Bulik-Sullivan, B., Stahl, E., et al. (2014). Partitioning heritability of regulatory and cell-type-specific variants across 11 common diseases. The American Journal of Human Genetics *95*, 535–552.

[11] Kichaev, G., Yang, W.-Y., Lindstrom, S., Hormozdiari, F., Eskin, E., Price, A. L., Kraft, P., and Pasaniuc, B. (2014). Integrating functional data to prioritize causal variants in statistical fine-mapping studies. PLoS Genetics *10*, e1004722

[12] Won, H.-H., Natarajan, P., Dobbyn, A., Jordan, D. M., Roussos, P., Lage, K., Raychaudhuri, S., Stahl, E., and Do, R. (2015). Disproportionate contributions of select genomic compartments and cell types to genetic risk for coronary artery disease. PLoS Genetics *11*, e1005622.

[13] Finucane, H. K., Bulik-Sullivan, B., Gusev, A., Trynka, G., Reshef, Y., Loh, P.-R., Anttila, V., Xu, H., Zang, C., Farh, K., et al. (2015). Partitioning heritability by functional annotation using genome-wide association summary statistics. Nature Genetics *47*, 1228–1235.

[14] Degner, J. F., Pai, A. A., Pique-Regi, R., Veyrieras, J.-B., Gaffney, D. J., Pickrell, J. K., De Leon, S., Michelini, K., Lewellen, N., Crawford, G. E., et al. (2012). Dnase [thinsp] i sensitivity qtls are a major determinant of human expression variation. Nature *482*, 390–394.

[15] McVicker, G., van de Geijn, B., Degner, J. F., Cain, C. E., Banovich, N. E., Raj, A., Lewellen, N., Myrthil, M., Gilad, Y., and Pritchard, J. K. (2013). Identification of genetic variants that affect histone modifications in human cells. Science *342*, 747–749.

[16] Kasowski, M., Kyriazopoulou-Panagiotopoulou, S., Grubert, F., Zaugg, J. B., Kundaje, A., Liu, Y., Boyle, A. P., Zhang, Q. C., Zakharia, F., Spacek, D. V., et al. (2013). Extensive variation in chromatin states across humans. Science *342*, 750–752.

[17] Kilpinen, H., Waszak, S. M., Gschwind, A. R., Raghav, S. K., Witwicki, R. M., Orioli, A., Migliavacca, E., Wiederkehr, M., Gutierrez-Arcelus, M., Panousis, N. I., et al. (2013). Coordinated effects of sequence variation on dna binding, chromatin structure, and transcription. Science *342*, 744–747.

[18] Waszak, S., Delaneau, O., Gschwind, A., Kilpinen, H., Raghav, S., Witwicki, R., Orioli, A., Wiederkehr, M., Panousis, N., Yurovsky, A., et al. (2015). Population variation and genetic control of modular chromatin architecture in humans. Cell *162*, 1039–1050.

[19] Taudt, A., Colome-Tatche, M., and Johannes, F. (2016). Genetic sources of population epigenomic variation. Nat Rev Genet *advance online publication*, –.

[20] Farh, K. K.-H., Marson, A., Zhu, J., Kleinewietfeld, M., Housley, W. J., Beik, S., Shoresh, N., Whitton, H., Ryan, R. J., Shishkin, A. A., et al. (2015). Genetic and epigenetic fine mapping of causal autoimmune disease variants. Nature *518*, 337–343.

[21] Moyerbrailean, G. A., Kalita, C. A., Harvey, C. T., Wen, X., Luca, F., and Pique-Regi, R. (2016). Which genetics variants in dnase-seq footprints are more likely to alter binding? PLoS Genetics *12*, e1005875.

[22] Gamazon, E. R., Wheeler, H. E., Shah, K. P., Mozaffari, S. V., Aquino-Michaels, K., Carroll, R. J., Eyler, A. E., Denny, J. C., Nicolae, D. L., Cox, N. J., et al. (2015). A gene-based association method for mapping traits using reference transcriptome data. Nature Genetics *47*, 1091–1098.

[23] Gusev, A., Ko, A., Shi, H., Bhatia, G., Chung, W., Penninx, B., Jansen, R., de Geus, E., Boomsma, D., Wright, F., et al. (2016). Integrative approaches for large-scale transcriptome-wide association studies. Nature Genetics *48*, 245–252.

[24] Zhu, Z., Zhang, F., Hu, H., Bakshi, A., Robinson, M., Powell, J., Montgomery, G., Goddard, M., Wray, N., Visscher, P., et al. (2016). Integration of summary data from gwas and eqtl studies predicts complex trait gene targets. Nature Genetics.

[25] Fromer, M., Roussos, P., Sieberts, S. K., Johnson, J. S., Kavanagh, D. H., Perumal, T. M., Ruderfer, D. M., Oh, E. C., Topol, A., Shah, H. R., et al. (2016). Gene expression elucidates functional impact of polygenic risk for schizophrenia. bioRxiv pp. 052209.

[26] Wright, F., Sullivan, P., Brooks, A., Zou, F., Sun, W., Xia, K., Madar, V., Jansen, R., Chung, W., Zhou, Y.-H., et al. (2014). Heritability and genomics of gene expression in peripheral blood. Nature Genetics *46*, 430–437.

[27] Li, Y., van+de+Geijn, B., Raj, A., Knowles, D., Petti, A., Golan, D., Gilad, Y., and Pritchard, J. (2016). Rna splicing is a primary link between genetic variation and disease. Science *352*, 600–604.

[28] Zhou, X., Carbonetto, P., and Stephens, M. (2013). Polygenic modeling with bayesian sparse linear mixed models. PLoS Genetics *9*, e1003264.

[29] Nica, A. C., Montgomery, S. B., Dimas, A. S., Stranger, B. E., Beazley, C., Barroso, I., and Dermitzakis, E. T. (2010). Candidate causal regulatory effects by integration of expression qtls with complex trait genetic associations. PLoS Genetics *6*, e1000895.

[30] Nicolae, D. L., Gamazon, E., Zhang, W., Duan, S., Dolan, M. E., and Cox, N. J. (2010). Trait-associated snps are more likely to be eqtls: annotation to enhance discovery from gwas. PLoS Genetics *6*, e1000888.

[31] Yang, J., Ferreira, T., Morris, A. P., Medland, S. E., Madden, P. A., Heath, A. C., Martin, N. G., Montgomery, G. W., Weedon, M. N., Loos, R. J., et al. (2012). Conditional and joint multiple-snp analysis of gwas summary statistics identifies additional variants influencing complex traits. Nature Genetics *44*, 369–375.

[32] Cross-Disorder Group of the Psychiatric Genomics Consortium. (2013). Genetic relationship between five psychiatric disorders estimated from genome-wide snps. Nature Genetics *45*, 984–994.

[33] Purcell, S. M., Wray, N. R., Stone, J. L., Visscher, P. M., O'Donovan, M. C., Sullivan, P. F., Sklar, P., Ruderfer, D. M., McQuillin, A., Morris, D. W., et al. (2009). Common polygenic variation contributes to risk of schizophrenia and bipolar disorder. Nature *460*, 748–752.

[34] Vilhjálmsson, B. J., Yang, J., Finucane, H. K., Gusev, A., Lindström, S., Ripke, S., Genovese, G., Loh, P.-R., Bhatia, G., Do, R., et al. (2015). Modeling linkage disequilibrium increases accuracy of polygenic risk scores. The American Journal of Human Genetics *97*, 576–592.

[35] Palla, L. and Dudbridge, F. (2015). A fast method that uses polygenic scores to estimate the variance explained by genome-wide marker panels and the proportion of variants affecting a trait. The American Journal of Human Genetics *97*, 250–259.

[36] Daetwyler, H. D., Villanueva, B., and Woolliams, J. A. (2008). Accuracy of predicting the genetic risk of disease using a genome-wide approach. PLoS one *3*, e3395.

[37] Haseman, J. and Elston, R. (1972). The investigation of linkage between a quantitative trait and a marker locus. Behavior Genetics *2*, 3–19.

[38] McCarthy, S. E., Makarov, V., Kirov, G., Addington, A. M., McClellan, J., Yoon, S., Perkins, D. O., Dickel, D. E., Kusenda, M., Krastoshevsky, O., et al. (2009). Microduplications of 16p11. 2 are associated with schizophrenia. Nature Genetics *41*, 1223–1227.

[39] Golzio, C., Willer, J., Talkowski, M. E., Oh, E. C., Taniguchi, Y., Jacquemont, S., Reymond, A., Sun, M., Sawa, A., Gusella, J. F., et al. (2012). Kctd13 is a major driver of mirrored neuroanatomical phenotypes of the 16p11. 2 copy number variant. Nature *485*, 363–367.

[40] Migliavacca, E., Golzio, C., Männik, K., Blumenthal, I., Oh, E. C., Harewood, L., Kosmicki, J. A., Loviglio, M. N., Giannuzzi, G., Hippolyte, L., et al. (2015). A potential contributory role for ciliary dysfunction in the 16p11. 2 600 kb bp4-bp5 pathology. The American Journal of Human Genetics *96*, 784–796.

[41] Maillard, A., Ruef, A., Pizzagalli, F., Migliavacca, E., Hippolyte, L., Adaszewski, S., Dukart, J., Ferrari, C., Conus, P., Männik, K., et al. (2015). The 16p11. 2 locus modulates brain structures common to autism, schizophrenia and obesity. Molecular psychiatry *20*, 140–147.

[42] Föcking, M., Lopez, L., English, J., Dicker, P., Wolff, A., Brindley, E., Wynne, K., Cagney, G., and Cotter, D. (2015). Proteomic and genomic evidence implicates the postsynaptic density in schizophrenia. Molecular psychiatry *20*, 424–432.

[43] Blizinsky, K. D., Diaz-Castro, B., Forrest, M. P., Schürmann, B., Bach, A. P., Martin-de Saavedra, M. D., Wang, L., Csernansky, J. G., Duan, J., and Penzes, P. (2016). Reversal of dendritic phenotypes in 16p11. 2 microduplication mouse model neurons by pharmacological targeting of a network hub. Proceedings of the National Academy of Sciences pp. 201607014.

[44] Akbarian, S., Liu, C., Knowles, J. A., Vaccarino, F. M., Farnham, P. J., Crawford, G. E., Jaffe, A. E., Pinto, D., Dracheva, S., Geschwind, D. H., et al. (2015). The psychencode project. Nature neuroscience *18*, 1707–1712.

[45] Reilly, S. K., Yin, J., Ayoub, A. E., Emera, D., Leng, J., Cotney, J., Sarro, R., Rakic, P., and Noonan, J. P. (2015). Evolutionary changes in promoter and enhancer activity during human corticogenesis. Science *347*, 1155–1159.

[46] Consortium, G. et al. (2015). The genotype-tissue expression (gtex) pilot analysis: Multitissue gene regulation in humans. Science *348*, 648–660.

[47] Pickrell, J. K., Marioni, J. C., Pai, A. A., Degner, J. F., Engelhardt, B. E., Nkadori, E., Veyrieras, J.-B., Stephens, M., Gilad, Y., and Pritchard, J. K. (2010). Understanding mechanisms underlying human gene expression variation with rna sequencing. Nature *464*, 768–772.

[48] Rosenberg, N. A., Huang, L., Jewett, E. M., Szpiech, Z. A., Jankovic, I., and Boehnke, M. (2010). Genome-wide association studies in diverse populations. Nature Reviews Genetics *11*, 356–366.

[49] Kichaev, G. and Pasaniuc, B. (2015). Leveraging functional-annotation data in trans-ethnic fine-mapping studies. The American Journal of Human Genetics *97*, 260–271.

[50] Bulik-Sullivan, B., Finucane, H. K., Anttila, V., Gusev, A., Day, F. R., Loh, P.-R., Duncan, L., Perry, J. R., Patterson, N., Robinson, E. B., et al. (2015). An atlas of genetic correlations across human diseases and traits. Nature Genetics.

[51] Sibley, C. R., Blazquez, L., and Ule, J. (2016). Lessons from non-canonical splicing. Nature Reviews Genetics.

[52] Nelson, C. E., Hakim, C. H., Ousterout, D. G., Thakore, P. I., Moreb, E. A., Rivera, R. M. C., Madhavan, S., Pan, X., Ran, F. A., Yan, W. X., et al. (2016). In vivo genome editing improves muscle function in a mouse model of duchenne muscular dystrophy. Science *351*, 403–407.

[53] Li, Y. I., Knowles, D. A., and Pritchard, J. K. (2016). Leafcutter: Annotation-free quantification of rna splicing. bioRxiv pp. 044107.

[54] Chen, C.-Y., Pollack, S., Hunter, D. J., Hirschhorn, J. N., Kraft, P., and Price, A. L. (2013). Improved ancestry inference using weights from external reference panels. Bioinformatics pp. btt144.

[55] Yang, J., Lee, S. H., Goddard, M. E., and Visscher, P. M. (2011). Gcta: a tool for genome-wide complex trait analysis. The American Journal of Human Genetics *88*, 76–82.

[56] Yang, J., Bakshi, A., Zhu, Z., Hemani, G., Vinkhuyzen, A. A., Lee, S. H., Robinson, M. R., Perry, J. R., Nolte, I. M., van Vliet-Ostaptchouk, J. V., et al. (2015). Genetic variance estimation with imputed variants finds negligible missing heritability for human height and body mass index. Nature Genetics.

[57] Liu, X., Finucane, H. K., Gusev, A., Bhatia, G., Gazal, S., O'Connor, L., Bulik-Sullivan, B., Wright, F., Sullivan, P., Neale, B., et al. (2016). Functional partitioning of local and distal gene expression regulation in multiple human tissues. bioRxiv.

[58] Consortium, U. et al. (2015). The uk10k project identifies rare variants in health and disease. Nature *526*, 82–90.

[59] Loh, P.-R., Danecek, P., Palamara, P. F., Fuchsberger, C., Reshef, Y. A., Finucane, H. K., Schoenherr, S., Forer, L., McCarthy, S., Abecasis, G. R., et al. (2016). Reference-based phasing using the haplotype reference consortium panel. bioRxiv pp. 052308.

LIST OF SUPPLEMENTARY MATERIALS

1 Supplementary Text
2 Table S1-S24
3 Figure S1-S38

Table 1: **Number of TWAS-associated genes across all phenotypes and tissues.**

	CMC/brain introns*	CMC/brain	NTR/blood	YFS/blood	MET/adipose	Total**
Heritable	(9,009) 3,890	5,514	2,743	5,418	4,654	11,749
SCZ associated	(80) 46	44	35	48	39	157
SCZ associated (joint†)	(21) 20	13	12	10	9	63
SCZ associated (novel)	(12) 10	9	6	6	7	35
SCZ associated (novel joint†)	(4) 4	4	3	4	2	17
Chromatin associated	(224) 125	244	182	346	232	806
SCZ and chromatin associated	(10) 8	11	10	13	7	42
Enrichment P-value	8.1e-05	2.0e-05	4.4e-04	6.5e-05	2.9e-02	1.4e-11

* Number of differentially spliced introns shown in parenthesis.

** Total number of unique gene associations.

† Significant in a summary-based joint analysis.

Table 2: **TWAS genes with association to schizophrenia and chromatin phenotypes.** 42 genes (including 7 genes at novel loci, highlighted with a [*]) had a significant TWAS association with SCZ and chromatin phenotypes. For each significant TWAS association with SCZ, the number of significant gene-chromatin associations (FWER 5% among TWAS gene-mark associations, by Bonforroni correction) are reported. In the middle columns '.' represents genes that were not heritable in the study and therefore not TWAS-associated. In the right columns '.' represents no identified association; genes with no chromatin associations are not shown. Top panel shows results from genes, with TSS listed as position; bottom panel shows results from differentially spliced introns in CMC with exon-exon junction listed as position (details in Table S9).

| Gene | Chr | Position | TWAS P-value | | | | Associated marks | | | | | |
			YFS/blood	MET/adipose	NTR/blood	CMC/brain	DHS	H3K27AC	H3K4ME1	H3K4ME3	PU1	RPB2
RERE	1	8,483,747	4e-07	2e-06	2e-06	.	.	.	.	.	.	3
SLC45A1	1	8,378,144	.	.	.	4e-08	.	.	.	.	.	1
MAP7D1*	1	36,621,565	6e-04	.	1e-06	.	.	.	.	.	.	1
MED8	1	43,855,483	5e-01	.	.	2e-06	.	.	1	.	.	.
ANP32E	1	150,207,026	.	.	1e-08	.	.	.	.	.	1	.
MRPS21	1	150,266,261	3e-06	3e-03	6e-03	2e-02	.	.	1	.	.	.
RFWD2*	1	176,176,380	4e-06	.	.	.	.	.	1	.	.	.
C2orf69	2	200,775,978	.	6e-10	.	.	.	.	.	1	.	.
GLT8D1	3	52,737,714	.	.	5e-08	3e-08	.	1	.	.	.	.
GLYCTK	3	52,321,835	2e-08	.	.	.	.	1	.	.	.	.
GNL3	3	52,719,935	7e-09	6e-07	.	5e-02	.	.	.	1	.	.
NEK4	3	52,804,965	.	.	.	2e-09	.	.	.	1	.	.
NT5DC2	3	52,567,793	6e-06	6e-06	.	7e-01	.	1	.	1	.	.
PPM1M	3	52,279,808	2e-07	2e-07	.	2e-03	.	1	.	.	.	.
TMEM110	3	52,931,597	1e-02	4e-01	1e-08	6e-06	.	1	1	2	.	.
PCCB	3	135,969,166	1e-08	1e-10	.	3e-10	1	.	3	.	.	.
RP11-53O19.3	5	44,826,178	.	6e-06	.	.	.	.	1	.	.	.
DND1	5	140,053,171	.	8e-07	1e-02	.	.	1	.	1	.	.
IK	5	140,027,383	4e-06	1e-06	.	5e-05	.	1	.	1	.	.
NDUFA2	5	140,027,370	2e-06	.	.	.	.	1	.	2	.	.
PCDHA2	5	140,174,443	.	.	.	7e-06	.	1	.	1	.	.
ZMAT2	5	140,080,031	5e-06	1e-03	.	3e-06	.	.	.	1	.	.
AS3MT	10	104,629,209	.	6e-08	7e-09	1e-05	.	1	.	.	.	.
MPHOSPH9	12	123,717,785	4e-09	1e-05	.	2e-08	.	1	.	.	1	.
KIAA0391*	14	35,591,526	7e-01	2e-07	5e-01	.	.	2	1	.	.	.
PPP2R3C*	14	35,591,748	6e-05	1e-01	3e-06	2e-02	.	2	2	.	.	.
MAPK3	16	30,134,630	5e-05	.	.	1e-06	.	1	.	.	.	1
GFOD2	16	67,753,273	.	.	6e-07	2e-05	.	1	.	2	.	.
TSNAXIP1	16	67,840,780	.	.	.	2e-06	.	.	1	2	.	.
DUS2L	16	68,038,024	1e-06	.	3e-06	4e-04	.	.	.	2	.	.
PRMT7	16	68,344,876	1e-05	8e-04	.	8e-06	.	.	1	1	.	.
GRAP*	17	18,950,336	.	.	5e-07	.	.	.	.	.	.	1
RNF112*	17	19,314,490	8e-06	.	.	.	.	.	.	.	.	1
ACTR5	20	37,377,096	2e-07	2e-04	.	7e-01	1	.	1	.	.	.
CBR3	21	37,507,262	6e-03	2e-03	2e-06	5e-04	1	.	2	.	.	.
CMC/brain splicing												
TBC1D5	3	17,255,862 - 17,279,655	.	.	.	3e-06	.	.	1	.	.	.
NEK4	3	52,800,010 - 52,800,194	.	.	.	1e-06	.	.	1	.	.	.
CCDC90B	11	82,985,783 - 82,991,184	.	.	.	3e-07	.	1	.	.	.	.
SBNO1	12	123,821,038 - 123,825,535	.	.	.	4e-10	.	.	.	.	1	.
KLC1	14	104,145,855 - 104,151,323	.	.	.	7e-12	.	.	1	1	.	.
RTN1*	14	60,074,210 - 60,193,637	.	.	.	1e-06	.	.	1	.	.	.
TAOK2	16	29,997,825 - 29,998,165	.	.	.	4e-06	.	.	.	.	.	1
PPP4C	16	30,094,168 - 30,094,715	.	.	.	2e-06	.	.	.	.	.	1

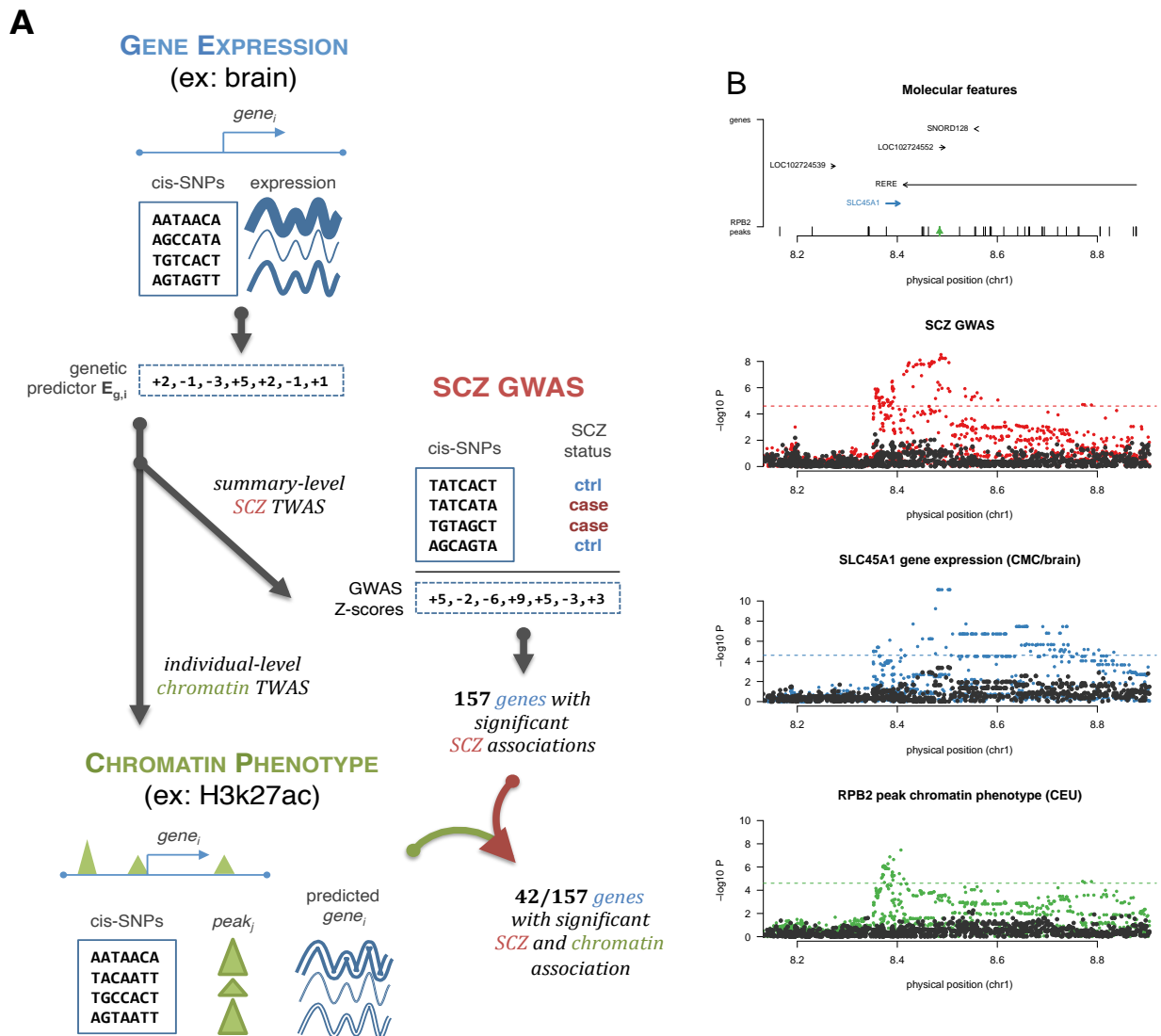* Novel, not overlapping 108 PGC SCZ GWAS loci

Figure 1: **Schematic and example of TWAS approach.** (**left**) Illustration of the TWAS approach: genetic predictor of gene expression (E_g is learned in a reference panel (top); integrated with SCZ GWAS association statistics to infer SCZ-E_g association (middle); further integrated with individual-level chromatin phenotypes to infer genes with SCZ and chromatin-E_g associations (bottom). (**right**) Example association of *SLC45A1* gene expression and SCZ, as well as *SLC45A1* expression and a distal RPB2 chromatin peak. Top panel shows locus schematic with all nearby genes and chromatin peaks and corresponding associations highlighted. Three lower panels show Manhattan plots of marginal association statistics before and after conditioning on the TWAS predicted expression (colored/dark dots, respectively). Dashed line shows local significance threshold after Bonferroni correction for number of SNPs. The full 1MB cis locus harbors 15 genes and 60 RPB2 peaks.
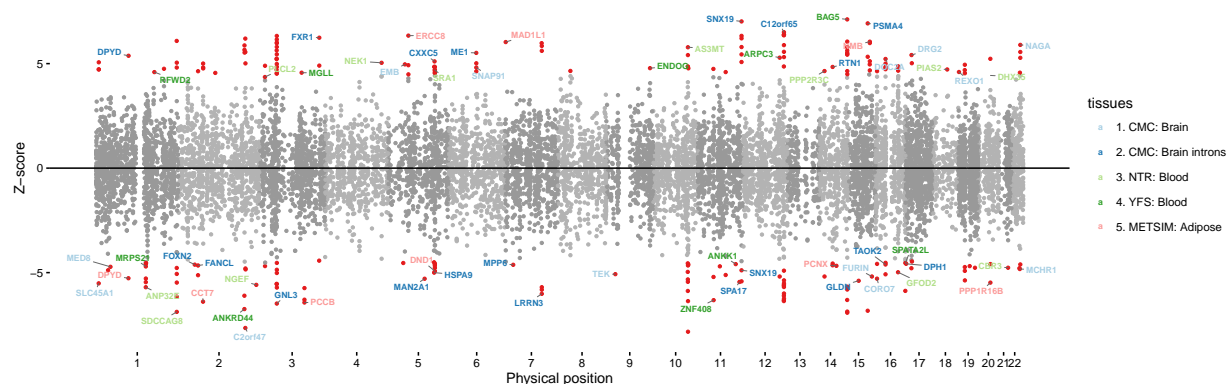
Figure 2: **Association between gene expression and schizophrenia.** Manhattan plot of SCZ TWAS associations across all tissues. Each point represents a single gene tested, with physical position plotted on x-axis and Z-score of association between gene and SCZ plotted on y-axis. Transcriptome-wide significant associations are highlighted as red points, with "clumped" independent associations (see Methods) labeled with gene names and color-coded by expression reference.
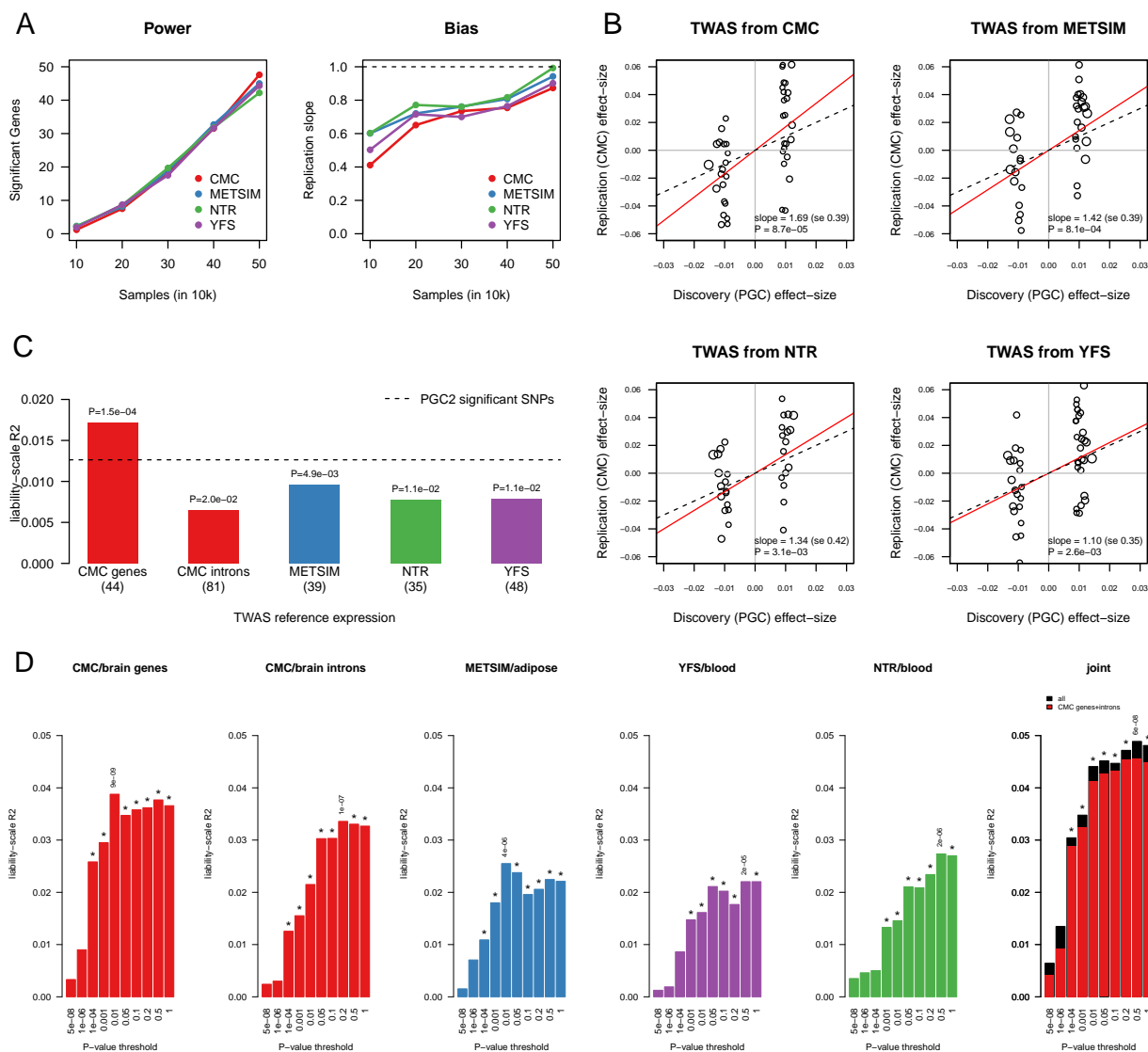
Figure 3: **Replication of TWAS associations.** (**a**) The PGC data was randomly split into increasingly large discovery samples (size on the x-axis) and TWAS statistics were estimated from each reference panel. Left panel reports the number of significant genes (after 5% FWER correction) for a given GWAS sample size. Right panel reports the slope from a regression of $\beta_{\text{replication}} \sim \beta_{\text{discovery}}$ for significant genes identified at each sample size (where all $56,000 - x$ remaining samples were used as replication). (**b**) TWAS effect-sizes for association to schizophrenia identified in the PGC (x-axis) compared to corresponding estimates in the CMC (y-axis). Dotted line corresponds to $y = x$; red line corresponds to the slope from a (Z-score weighted) regression of CMC $\sim$ PGC, with estimate and p-value shown in bottom right. (**c**) Schizophrenia risk prediction R^2 shown for risk scores constructed from significant TWAS genes (bars) and PGC2 GWAS SNPs (dashed line, comparable to the $1\% - 3\%$ reported in ref[1]). Number of genes used in each score reported in parenthesis. Linear-regression R^2 of phenotype on predictor (after subtracting R^2 from jointly fit ancestry PCs) was transformed to the liability scale assuming schizophrenia prevalence of 1%, a linear transformation consistent across all predictors. (**d**) Schizophrenia risk prediction R^2 for polygenic gene risk scores across multiple significance thresholds. Significant correlations (after Bonferroni correction for number of thresholds tested) are indicated with a (*) and most significant P-value reported. Right-most panel shows prediction from all tissues jointly (black) and from CMC/brain genes + differentially expressed introns jointly (red).
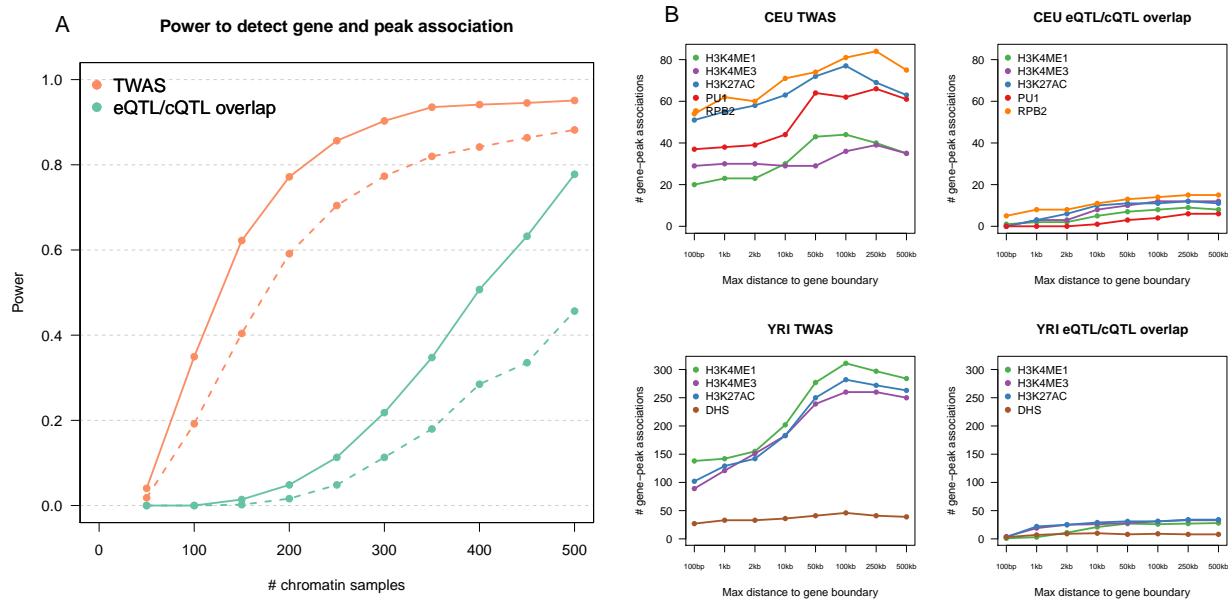
Figure 4: **Power and detection of significant gene-mark associations.** (**a**) Molecular phenotypes were simulated under the SNP → chromatin → expression model and two methods to detect gene-mark associations evaluated. (TWAS, orange) corresponds to predicting expression from a held-out reference panel with 1,000 individuals and testing each proximal chromatin peak for association. (eQTL/cQTL, green) corresponds to identifying SNPs that are significantly associated with both chromatin and expression at the locus. For a given chromatin phenotype sample size (x-axis), power was measured as the number of instances where locus was deemed significant after accounting for number of gene-mark pairs tested (TWAS) or number of SNPs and gene-mark pairs tested (eQTL/cQTL). Solid (dashed) lines correspond to 1 (2) chromatin-causing variants in the simulation. (**b**) Genes significantly associated with a chromatin phenotype peak in YRI/CEU. For a given distance from the gene (x-axis), the number of unique genes is reported after experiment-wide Bonferroni correction for tests across all chromatin phenotypes. Results from TWAS prediction-based approach shown on left; results from overlapping QTL approach on the right (see Methods).